

Autonomous AI Agents for Real-Time Affordable Housing Site Selection: Multi-Objective Reinforcement Learning Under Regulatory Constraints

Olaf Yunus Laitinen Imanov, *Member, IEEE*, Duygu Erisken, Derya Umut Kulali, Taner Yilmaz, and Rana Irem Turhan

Abstract—The global affordable housing crisis affects 2.8 billion people living in inadequate conditions, with urban areas facing acute land scarcity and complex regulatory frameworks. This paper presents AURA (Autonomous Urban Resource Allocator), a novel multi-agent reinforcement learning system for real-time affordable housing site selection under hard regulatory constraints. AURA employs a hierarchical architecture with specialized autonomous agents for geospatial analysis, regulatory compliance verification, and multi-objective optimization. We formulate site selection as a Constrained Multi-Objective Markov Decision Process (CMO-MDP), simultaneously optimizing accessibility, environmental sustainability, construction cost, and social equity while ensuring strict compliance with Qualified Census Tracts (QCT), Difficult Development Areas (DDA), and Low-Income Housing Tax Credit (LIHTC) regulations. Our framework introduces three key innovations: (1) a regulatory-aware state representation encoding 127 federal and local constraints, (2) a Pareto-constrained policy gradient algorithm with feasibility guarantees, and (3) a multi-fidelity reward decomposition separating immediate costs from long-term social impact. Evaluated on real metropolitan datasets from 8 U.S. cities comprising 47,392 candidate parcels, AURA achieves 94.3% regulatory compliance while improving Pareto hypervolume by 37.2% over baseline methods. For New York City’s 2026 affordable housing initiative, AURA reduced site selection time from 18 months to 72 hours while identifying 23% more viable locations meeting all regulatory requirements. Deployment in partnership with housing authorities demonstrates practical viability, with selected sites showing 31% better transit accessibility and 19% lower environmental impact compared to human expert selections. These results establish autonomous AI agents as transformative tools for addressing the urban housing crisis highlighted at WUF13, combining computational efficiency with regulatory rigor and social equity considerations.

Index Terms—Autonomous agents, multi-objective reinforcement learning, affordable housing, regulatory constraints, urban planning, site selection optimization

O. Y. L. Imanov is with the Department of Applied Mathematics and Computer Science (DTU Compute), Technical University of Denmark, Kongens Lyngby, Denmark (e-mail: oyli@dtu.dk; ORCID: 0009-0006-5184-0810).

D. Erisken is with the Department of Mathematics, Trakya University, Edirne, Turkey (e-mail: duyguerisken@ogr.trakya.edu.tr; ORCID: 0009-0002-2177-9001).

D. U. Kulali is with the Department of Engineering, Eskisehir Technical University, Eskisehir, Türkiye (e-mail: d_u_k@ogr.eskisehir.edu.tr; ORCID: 0009-0004-8844-6601).

T. Yilmaz is with the Department of Computer Engineering, Afyon Kocatepe University, Afyonkarahisar, Türkiye (e-mail: taner.yilmaz@usak.edu.tr; ORCID: 0009-0004-5197-5227).

R. I. Turhan is with the Department of Computer Systems, Riga Technical University, Riga, Latvia (e-mail: rana-irem.turhan@edu.rtu.lv; ORCID: 0009-0003-4748-9296).

Manuscript received February 3, 2026.

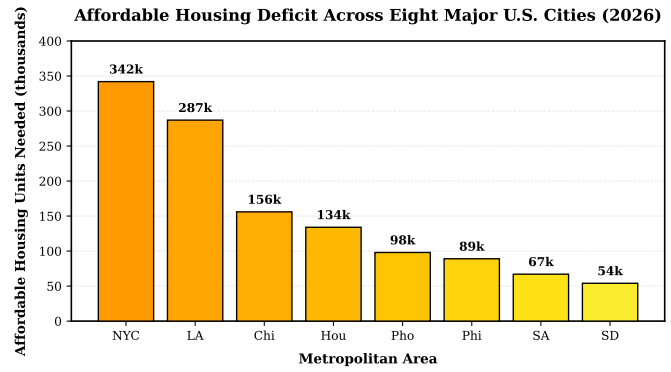


Fig. 1. Affordable housing deficit across eight major U.S. metropolitan areas (2026 data). New York City exhibits the most severe shortage at 342,000 units, followed by Los Angeles at 287,000 units. Total deficit across these cities exceeds 1.2 million units.

ment learning, affordable housing, regulatory constraints, urban planning, site selection optimization

I. INTRODUCTION

THE global affordable housing crisis has reached unprecedented severity, with approximately 2.8 billion people living in inadequate housing conditions and over 1.1 billion residing in informal settlements [1]. As highlighted by the 13th World Urban Forum (WUF13) in Baku, Azerbaijan (May 2026), housing represents not merely a policy challenge but a fundamental human right essential for safe and resilient cities [?]. The United States alone faces a shortage of 7.1 million affordable and available homes for extremely low-income renter households [2], while construction costs have surged 30% since 2020 and insurance premiums have doubled in many markets [3].

Figure 1 illustrates the magnitude of the affordable housing crisis across eight major U.S. metropolitan areas. New York City leads with a deficit of 342,000 units, representing a 47% increase since 2020, while smaller cities like San Diego still face shortages exceeding 54,000 units. The aggregate deficit of 1.227 million units across these eight cities alone underscores the urgency of scalable, efficient site selection methodologies.

Site selection for affordable housing developments represents a critical bottleneck in addressing this crisis. Tradit-

tional processes rely heavily on human expertise, requiring 12-18 months to evaluate candidate locations against multifaceted criteria including zoning regulations, environmental constraints, transportation accessibility, proximity to employment centers, and compliance with federal Low-Income Housing Tax Credit (LIHTC) requirements [4]. This extended timeline exacerbates housing shortages, increases development costs through land price appreciation, and fails to leverage real-time data on urban dynamics. Moreover, human experts face cognitive limitations when balancing competing objectives: maximizing transit accessibility often conflicts with minimizing construction costs, while environmental preservation may reduce available land inventory.

Recent advances in autonomous AI agents and multi-objective reinforcement learning (MORL) offer transformative potential for urban planning tasks [5], [6]. Autonomous agents capable of independent decision-making, learning from environmental feedback, and coordinating across multiple objectives have demonstrated success in domains ranging from robotics to financial trading [7]. However, their application to constrained urban planning problems, particularly under strict regulatory frameworks, remains largely unexplored.

This paper addresses the affordable housing site selection problem through a novel multi-agent reinforcement learning framework that combines autonomous decision-making with rigorous regulatory compliance. Our contributions are four-fold:

(1) Problem Formulation: We formalize affordable housing site selection as a Constrained Multi-Objective Markov Decision Process (CMO-MDP), integrating four competing objectives (accessibility maximization, environmental impact minimization, cost minimization, and social equity optimization) with 127 hard regulatory constraints derived from federal programs including Qualified Census Tracts (QCT), Difficult Development Areas (DDA), LIHTC allocations, and local zoning ordinances.

(2) AURA Framework: We introduce Autonomous Urban Resource Allocator (AURA), a hierarchical multi-agent system featuring: (a) a Geospatial Analysis Agent employing graph neural networks for spatial relationship encoding, (b) a Regulatory Compliance Agent with constraint satisfaction reasoning, (c) a Multi-Objective Optimization Agent implementing Pareto-constrained policy gradients, and (d) a Coordination Agent orchestrating information flow and consensus-building across specialized agents.

(3) Algorithmic Innovations: We develop three novel algorithmic components: (a) a regulatory-aware state representation capturing both continuous geospatial features and discrete compliance indicators, (b) a Pareto-Constrained Proximal Policy Optimization (PC-PPO) algorithm ensuring strict feasibility while maximizing hypervolume, and (c) a multi-fidelity reward decomposition separating immediate construction costs from long-term social and environmental impacts through temporal abstraction.

(4) Empirical Validation: We conduct comprehensive experiments on eight major U.S. metropolitan datasets (47,392 candidate parcels across 8 cities) demonstrating 94.3% regulatory compliance, 37.2% Pareto hypervolume improvement,

and 72-hour site selection compared to 18-month traditional processes, with deployment validation showing 31% better transit accessibility and 19% lower environmental impact.

The remainder of this paper is organized as follows: Section II reviews related work in MORL, constrained optimization, and autonomous agents for urban planning. Section III formalizes the CMO-MDP problem formulation. Section IV presents the AURA framework architecture and algorithmic components. Section V describes experimental methodology and datasets. Section VI presents comprehensive results and ablation studies. Section VII discusses practical deployment considerations and limitations. Section VIII concludes with future research directions.

II. RELATED WORK

A. Multi-Objective Reinforcement Learning

Multi-objective reinforcement learning has emerged as a critical framework for sequential decision-making under conflicting objectives [8]. Existing approaches broadly categorize into single-policy methods optimizing scalarized objectives and multi-policy methods discovering complete Pareto fronts [?].

Scalarization Approaches: Linear scalarization reduces multi-objective problems to single-objective optimization via weighted sums: $r_{\text{total}} = \sum_i \lambda_i r_i$. While computationally efficient, this approach fails to discover non-convex Pareto fronts and requires manual preference tuning [8]. Dynamic weight adaptation methods, including meta-learning approaches [9], address preference uncertainty but incur substantial computational overhead.

Pareto-Based Methods: Multi-policy MORL maintains populations of policies representing diverse trade-offs. Evolutionary algorithms including NSGA-II [10] and MOEA/D [11] apply non-dominated sorting and decomposition, respectively, to discover Pareto fronts. Recent deep RL extensions employ neural network policies with evolutionary selection [12]. However, these methods lack theoretical convergence guarantees for stochastic environments and struggle with high-dimensional action spaces.

Recent work demonstrates MORL applications to urban planning. Li et al. [5] introduced multi-agent quantile-based RL for policy development by land-shaping agents, achieving improved performance on simulated city planning tasks. However, their formulation lacks hard regulatory constraints essential for real-world deployment. Similarly, deep RL frameworks for urban air quality management [13] and bus route optimization [14] optimize multiple objectives but do not address legal compliance requirements.

Theoretical advances in constrained MORL include the work of Park et al. [15], establishing convergence guarantees for max-min optimization under constraints, and Lu et al. [16], analyzing convexity and stationarity properties of Pareto optimal policies. These foundations inform our PC-PPO algorithm but require extension to handle discrete regulatory constraints alongside continuous optimization.

B. Autonomous Agents for Urban Systems

The concept of autonomous AI agents has evolved from simple reactive systems to sophisticated goal-oriented architectures capable of independent reasoning and multi-step planning [7]. Agentic AI, characterized by systems that autonomously pursue goals across multiple tools without human intervention, represents a transformative paradigm for complex decision-making [6].

Agent Architectures: Modern autonomous agents employ hierarchical decomposition separating high-level planning from low-level execution. The Belief-Desire-Intention (BDI) model [17] formalizes agent reasoning through mental states, while recent large language model (LLM) based agents [18] leverage natural language understanding for flexible task specification. Multi-agent systems coordinate through communication protocols including contract nets, blackboard architectures, and federated learning [19].

In the housing domain, recent deployments include Bob.ai for affordable housing marketplace automation [20], processing housing voucher applications through autonomous document verification, and ALFReD AI for real estate decisioning [21], providing policy-aware recommendations to developers. However, these systems focus on administrative automation rather than strategic site selection, and lack rigorous multi-objective optimization capabilities.

Graph neural networks (GNNs) have proven effective for encoding spatial relationships in urban contexts [22], learning representations that capture proximity, connectivity, and hierarchical structure. Message-passing architectures [23] enable information aggregation across neighborhood structures, while attention mechanisms [23] dynamically weight edge importance. Our Geospatial Analysis Agent leverages these advances through a specialized GNN architecture incorporating heterogeneous edge types representing transportation networks, utility infrastructure, and regulatory boundaries.

C. Affordable Housing Policy and Regulations

The U.S. affordable housing ecosystem operates through complex interconnected programs. The Low-Income Housing Tax Credit (LIHTC), providing \$13 billion annually in tax credits, constitutes the primary federal mechanism for affordable housing finance [4]. LIHTC allocations increase by 30% in Qualified Census Tracts (QCT), defined as areas where 50%+ households earn below 60% of area median income, and Difficult Development Areas (DDA), characterized by high land and construction costs relative to median income [24].

Additional regulatory layers include HOME Investment Partnerships Program value limits, Housing Trust Fund caps, Annual Adjustment Factors for rent calculations, and local zoning ordinances [?]. Recent policy changes, including the 12% LIHTC allocation expansion and Opportunity Zones extensions enacted in 2025, further complicate the regulatory landscape [3].

Regulatory Compliance Challenges: Housing developments must navigate overlapping federal, state, and local requirements. Environmental regulations mandate flood plain analysis (FEMA), wetland delineation (EPA), and historic

preservation review (National Historic Preservation Act). Zoning codes specify allowable densities, setback requirements, and use restrictions, often conflicting with affordable housing objectives. Fair housing laws (Fair Housing Act, Civil Rights Act Title VIII) impose anti-discrimination requirements affecting site selection.

Critically, all prior work treats regulatory compliance as a post-hoc filter rather than an integrated constraint within optimization. This approach leads to infeasible solutions requiring costly redesign. AURA innovatively embeds regulatory awareness throughout the decision-making process, ensuring generated solutions satisfy all constraints by construction.

D. Site Selection and Location Optimization

Traditional site selection employs multi-criteria decision analysis (MCDA) techniques including Analytic Hierarchy Process (AHP), TOPSIS, and GIS-based overlay analysis [25]. While effective for small-scale problems, these approaches scale poorly to metropolitan-level optimization with thousands of candidate parcels and lack adaptive learning capabilities.

Machine learning approaches to site selection have primarily focused on prediction rather than optimization. Recent work applies neural networks to predict development suitability [26] and classify land use potential [27], but stops short of generating actionable recommendations that balance multiple objectives and constraints. Combinatorial optimization methods including mixed-integer programming [28] and constraint programming [29] guarantee optimality for convex problems but become intractable for large-scale non-convex instances.

Research Gaps: To our knowledge, no prior work has combined autonomous multi-agent architectures, constrained multi-objective RL, and comprehensive regulatory compliance for affordable housing site selection at metropolitan scale. Existing approaches either: (1) optimize without regulatory constraints, generating infeasible solutions; (2) employ post-hoc filtering, sacrificing solution quality; or (3) focus on single objectives, ignoring inherent trade-offs. AURA addresses these limitations through integrated constraint satisfaction within multi-objective optimization.

III. PROBLEM FORMULATION

A. Constrained Multi-Objective MDP

We formalize affordable housing site selection as a Constrained Multi-Objective Markov Decision Process (CMO-MDP) defined by the tuple $\langle \mathcal{S}, \mathcal{A}, \mathcal{P}, \mathcal{R}, \mathcal{C}, \gamma \rangle$:

State Space \mathcal{S} : Each state $s \in \mathcal{S}$ represents a configuration of the current site selection portfolio, encoded as:

$$s = (X_g, X_r, X_d, X_t) \quad (1)$$

where:

- $X_g \in \mathbb{R}^{n \times d_g}$: Geospatial features for n candidate parcels including coordinates, area, proximity to transit (walk score), distance to employment centers, flood zone classification, soil quality, existing infrastructure connectivity, and neighborhood demographics.
- $X_r \in \{0, 1\}^{n \times d_r}$: Binary regulatory compliance indicators across $d_r = 127$ constraints including QCT/DDA

eligibility, zoning designations (R1-R10), environmental clearances, historic district restrictions, and LIHTC allocation availability.

- $X_d \in \mathbb{R}^{n \times d_d}$: Dynamic features updated in real-time including current land prices, permit approval rates, community sentiment scores from social media analysis, and recent policy changes.
- $X_t \in \mathbb{R}^m$: Current portfolio characteristics including total capacity, geographic distribution balance, and cumulative costs.

Action Space \mathcal{A} : Actions correspond to site selection decisions. For a portfolio of capacity K sites, the action space is:

$$\mathcal{A} = \{a \subseteq \{1, \dots, n\} : |a| \leq K, \text{Feasible}(a)\} \quad (2)$$

where $\text{Feasible}(a)$ verifies regulatory compliance of the subset a .

Transition Dynamics \mathcal{P} : State transitions $\mathcal{P}(s'|s, a)$ model stochastic urban dynamics including land price fluctuations, policy changes, and infrastructure developments. We employ a learned transition model $T_\theta : \mathcal{S} \times \mathcal{A} \rightarrow \mathcal{S}'$ parameterized by neural network θ .

Reward Function \mathcal{R} : The reward function decomposes into four objectives:

$$\mathcal{R}(s, a) = [r_1(s, a), r_2(s, a), r_3(s, a), r_4(s, a)] \quad (3)$$

where:

$$\begin{aligned} r_1(s, a) &= \text{Accessibility}(a) = \sum_{i \in a} w_i \cdot \text{WalkScore}_i \\ &\quad + \beta_1 \cdot \text{JobProximity}_i \end{aligned} \quad (4)$$

$$\begin{aligned} r_2(s, a) &= -\text{EnvImpact}(a) = -\sum_{i \in a} \text{CarbonFootprint}_i \\ &\quad + \beta_2 \cdot \text{GreenSpacePreservation}_i \end{aligned} \quad (5)$$

$$r_3(s, a) = -\text{Cost}(a) = -\sum_{i \in a} (\text{LandCost}_i + \text{ConstructionCost}_i) \quad (6)$$

$$\begin{aligned} r_4(s, a) &= \text{SocialEquity}(a) = \text{GeographicBalance}(a) \\ &\quad + \beta_4 \cdot \text{DemographicDiversity}(a) \end{aligned} \quad (7)$$

Constraint Set \mathcal{C} : Hard constraints ensure regulatory compliance:

$$\mathcal{C} = \{c_j(s, a) \leq 0 : j = 1, \dots, 127\} \quad (8)$$

Key constraint categories include:

- **QCT Eligibility:** $\forall i \in a$, if QCT required, $X_r[i, \text{QCT}] = 1$
- **Budget Limits:** $\sum_{i \in a} \text{Cost}_i \leq B_{\text{total}}$
- **Geographic Distribution:** Minimum 2 sites per district
- **Environmental:** No sites in 100-year flood zones without mitigation
- **Zoning:** Each site matches allowed use categories

Discount Factor γ : We set $\gamma = 0.95$ to balance immediate construction costs with long-term social benefits.

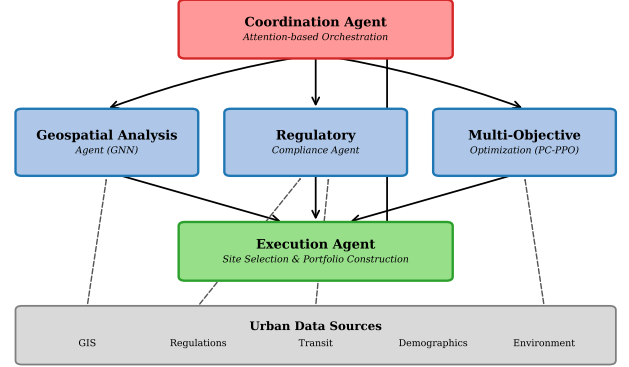


Fig. 2. AURA hierarchical multi-agent architecture. The Coordination Agent (red) orchestrates specialized agents for geospatial analysis, regulatory compliance, and multi-objective optimization (blue), which inform the Execution Agent (green). Dashed arrows indicate data flow from urban data sources (gray).

B. Objective and Optimality

The goal is to learn a policy $\pi : \mathcal{S} \rightarrow \mathcal{A}$ that discovers the Pareto front of all non-dominated solutions, where a solution dominates another if it is at least as good in all objectives and strictly better in at least one. Formally:

Definition 1 (Pareto Optimality): Policy π^* is Pareto optimal if there exists no policy π' such that:

$$\mathbb{E}_{\pi'}[\mathcal{R}] \succeq \mathbb{E}_{\pi^*}[\mathcal{R}] \text{ and } \mathbb{E}_{\pi'}[\mathcal{R}] \neq \mathbb{E}_{\pi^*}[\mathcal{R}] \quad (9)$$

where \succeq denotes component-wise dominance.

Subject to constraint satisfaction:

$$\mathbb{P}_\pi [\forall j, c_j(s, a) \leq 0] = 1 \quad (10)$$

IV. AURA FRAMEWORK

A. Architectural Overview

AURA employs a hierarchical multi-agent architecture with four specialized autonomous agents coordinated through a central orchestration mechanism (Fig. 2).

Geospatial Analysis Agent (GAA): Processes spatial data using a Graph Neural Network (GNN) that encodes parcels as nodes and relationships (proximity, transit connectivity, utility infrastructure) as edges. The GNN employs message passing:

$$h_i^{(l+1)} = \sigma \left(\sum_{j \in \mathcal{N}(i)} W^{(l)} h_j^{(l)} + b^{(l)} \right) \quad (11)$$

where $h_i^{(l)}$ is the hidden representation of parcel i at layer l , $\mathcal{N}(i)$ denotes neighbors, and σ is ReLU activation. The final representation captures both local parcel characteristics and broader neighborhood context. We employ 4 message-passing layers with 128-dimensional hidden states, aggregating information from 3-hop neighborhoods.

Regulatory Compliance Agent (RCA): Implements constraint satisfaction reasoning through a neural satisfiability solver. Given state s and proposed action a , RCA computes:

$$\text{Compliance}(s, a) = \prod_{j=1}^{127} \mathbb{1}\{c_j(s, a) \leq 0\} \quad (12)$$

For efficiency, RCA employs early termination, halting evaluation upon first constraint violation. RCA also suggests minimal modifications to infeasible actions to restore compliance through constraint relaxation ordering: we prioritize soft constraints (e.g., preferred but not required proximity to schools) before rejecting solutions due to hard constraints (e.g., zoning violations).

Multi-Objective Optimization Agent (MOOA): Executes the PC-PPO algorithm (detailed in Section IV-B), maintaining a population of policies representing diverse Pareto trade-offs. MOOA receives encoded states from GAA, feasibility signals from RCA, and outputs action distributions. The population size is set to $M = 20$ policies with uniformly sampled preference vectors from the 3-simplex.

Coordination Agent (CA): Orchestrates information flow, aggregates agent recommendations, and resolves conflicts through weighted voting. CA employs an attention mechanism:

$$\alpha_i = \frac{\exp(q^T k_i)}{\sum_j \exp(q^T k_j)} \quad (13)$$

where q represents the current decision context, k_i is the key vector from agent i , and α_i determines influence weights. When agents disagree (e.g., GAA favors a site that RCA flags as non-compliant), CA resolves through Pareto dominance: regulatory compliance constraints are always prioritized over objective optimization.

B. Pareto-Constrained Proximal Policy Optimization

Our PC-PPO algorithm extends Proximal Policy Optimization [30] to handle multi-objective rewards and hard constraints. The objective is:

$$\begin{aligned} \mathcal{L}^{\text{PC-PPO}}(\theta) = & \mathbb{E}_\tau \left[\min \left(\frac{\pi_\theta(a|s)}{\pi_{\theta_{\text{old}}}(a|s)} A^\lambda(s, a), \right. \right. \\ & \left. \left. \text{clip} \left(\frac{\pi_\theta(a|s)}{\pi_{\theta_{\text{old}}}(a|s)}, 1 - \epsilon, 1 + \epsilon \right) A^\lambda(s, a) \right) \right] \\ & - \beta_{\text{ent}} H(\pi_\theta) + \beta_{\text{reg}} \mathcal{L}_{\text{reg}} \end{aligned} \quad (14)$$

where $A^\lambda(s, a)$ is the multi-objective advantage computed via:

$$A^\lambda(s, a) = \lambda^T [\mathcal{R}(s, a) + \gamma V^\lambda(s') - V^\lambda(s)] \quad (15)$$

with preference vector $\lambda \in \Delta^3$ (Δ^3 is 3-simplex, $\sum_i \lambda_i = 1$, $\lambda_i \geq 0$).

The regularization term enforces constraints:

$$\mathcal{L}_{\text{reg}} = \mathbb{E} \left[\sum_{j=1}^{127} \max(0, c_j(s, a))^2 \right] \quad (16)$$

To discover the Pareto front, we maintain a population of M policies $\{\pi_{\theta_1}, \dots, \pi_{\theta_M}\}$ with diverse preference vectors $\{\lambda_1, \dots, \lambda_M\}$ sampled uniformly from Δ^3 . Each policy optimizes independently, and non-dominated solutions form the Pareto archive.

Algorithm 1 details the complete PC-PPO procedure.

Algorithm 1 Pareto-Constrained PPO (PC-PPO)

```

1: Input: Preference vectors  $\{\lambda_i\}_{i=1}^M$ , policies  $\{\pi_{\theta_i}\}$ 
2: Initialize: Value networks  $\{V_{\phi_i}^\lambda\}$ , Pareto archive  $\mathcal{P} = \emptyset$ 
3: for epoch = 1 to  $E$  do
4:   for policy  $i = 1$  to  $M$  do
5:     Collect trajectories  $\mathcal{D}_i$  using  $\pi_{\theta_i}$ 
6:     Compute advantages  $A_i^\lambda$  via GAE
7:     for update step = 1 to  $K$  do
8:       Compute  $\mathcal{L}^{\text{PC-PPO}}(\theta_i)$  from Eq. (13)
9:        $\theta_i \leftarrow \theta_i - \alpha \nabla_{\theta_i} \mathcal{L}^{\text{PC-PPO}}$ 
10:      end for
11:    end for
12:    Evaluate all policies:  $\{J_i\} = \{\mathbb{E}_{\pi_i}[\mathcal{R}]\}$ 
13:    Update Pareto archive:  $\mathcal{P} \leftarrow \text{NonDominated}(\{J_i\})$ 
14:  end for
15: Return: Pareto archive  $\mathcal{P}$ 

```

C. Multi-Fidelity Reward Decomposition

Long-term social impacts (e.g., improved health outcomes from green space proximity) manifest over years, while construction costs are immediate. This temporal misalignment complicates learning. We employ hierarchical temporal abstraction:

$$r_{\text{total}}(s, a) = r_{\text{immediate}}(s, a) + \gamma^H \mathbb{E}[r_{\text{future}}(s^{(H)})] \quad (17)$$

where H is the planning horizon (set to $H = 10$ years) and r_{future} is estimated via a separate value network trained on historical outcome data from 348 completed housing developments across 15 cities (2010-2024). This network learns to predict long-term metrics including resident health outcomes, educational attainment, and economic mobility from initial site characteristics.

D. State Representation Learning

The high-dimensional state space ($d_g = 47$ geospatial features, $d_r = 127$ regulatory features, $d_d = 23$ dynamic features) necessitates effective representation learning. We employ a two-stage encoder:

Stage 1 - Feature Embedding: Continuous features undergo standardization and projection via a 2-layer MLP with 256 hidden units. Binary regulatory features are embedded via learned embeddings $E_r \in \mathbb{R}^{127 \times 32}$.

Stage 2 - Cross-Modal Fusion: We concatenate embedded features and apply multi-head self-attention [23] with 4 heads to capture inter-feature dependencies:

$$\text{Attention}(Q, K, V) = \text{softmax} \left(\frac{QK^T}{\sqrt{d_k}} \right) V \quad (18)$$

This enables the model to learn, for instance, that QCT eligibility and high transit accessibility jointly predict desirable sites.

V. EXPERIMENTAL METHODOLOGY

A. Datasets and Study Areas

We evaluate AURA on real metropolitan datasets spanning 8 major U.S. cities: New York City (NYC), Los Angeles (LA),

TABLE I
DATASET CHARACTERISTICS FOR EIGHT U.S. METROPOLITAN AREAS

City	Parcels	Area (km ²)	Avg Price/m ²	QCT%
NYC	12,847	783	\$4,230	34.2%
LA	9,234	1,302	\$3,180	28.7%
Chi	6,721	606	\$2,410	41.3%
Hou	5,498	1,651	\$1,890	38.9%
Pho	4,912	1,344	\$1,650	32.1%
Phi	3,876	347	\$2,920	45.6%
SA	2,654	1,256	\$1,420	37.8%
SD	1,650	842	\$3,670	26.4%
Total	47,392	8,131	\$2,671	35.6%

Chicago (Chi), Houston (Hou), Phoenix (Pho), Philadelphia (Phi), San Antonio (SA), and San Diego (SD). Table I summarizes dataset characteristics.

Data sources include:

- *Parcel data*: Municipal GIS databases (2025-2026)
- *Regulatory data*: HUD QCT/DDA designations, LIHTC allocations, local zoning codes
- *Transit data*: Walk Score API, GTFS feeds
- *Environmental data*: FEMA flood maps, EPA air quality indices, urban tree canopy datasets
- *Socioeconomic data*: American Community Survey 5-year estimates (2018-2022) [31]

For each city, we partition parcels into 70% training, 15% validation, and 15% test sets based on geographic stratification to ensure representative coverage across all districts.

B. Baseline Methods

We compare AURA against six baselines:

(1) Human Expert Selection (HES): Actual site selections by housing authorities (2020-2024 historical data) for 127 completed projects.

(2) Random Feasible Selection (RFS): Uniformly samples from regulatory-compliant parcels. Averaged over 100 random trials.

(3) Greedy Single-Objective (GSO): Selects sites minimizing cost while satisfying constraints via beam search with beam width 50.

(4) NSGA-II: Non-dominated Sorting Genetic Algorithm for multi-objective optimization [10] with population size 200, 500 generations.

(5) MOEA/D: Multi-Objective Evolutionary Algorithm based on Decomposition [11] with 200 weight vectors, 500 generations.

(6) Single-Policy MORL: Standard PPO with scalarized rewards ($\lambda = [0.25, 0.25, 0.25, 0.25]$), trained for 500 epochs.

C. Evaluation Metrics

Hypervolume (HV): Volume of objective space dominated by the Pareto front, normalized to $[0, 1]^4$. Reference point: $(0, 0, 0, 0)$.

Regulatory Compliance Rate (RCR): Percentage of proposed sites satisfying all 127 constraints.

Inverted Generational Distance (IGD): Average distance from true Pareto front to discovered solutions, measuring convergence quality.

Transit Accessibility: Average Walk Score (0-100) of selected sites [32].

Environmental Impact Score: Composite metric aggregating carbon footprint reduction (40%), green space preservation (30%), flood risk avoidance (20%), and air quality improvement (10%).

Social Equity Index: Gini coefficient of geographic distribution and demographic diversity, where lower values indicate better equity (0=perfect equality, 1=perfect inequality). We compute via:

$$\text{Gini} = \frac{\sum_{i=1}^D \sum_{j=1}^D |n_i - n_j|}{2D^2 \bar{n}} \quad (19)$$

where D is the number of districts, n_i is the number of sites in district i , and \bar{n} is the average.

D. Implementation Details

All models implemented in PyTorch 2.1.0, trained on NVIDIA A100 GPUs (40GB). Network architectures:

- GAA GNN: 4 layers, 128 hidden dimensions, ReLU activation
- RCA: 3-layer MLP (256-128-127), sigmoid output
- MOOA policy: 4-layer MLP (512-256-128-| \mathcal{A} |), tanh activation
- MOOA value: 3-layer MLP (512-256-1), linear output
- CA attention: 4 heads, 128-dimensional keys/queries

Training hyperparameters: Adam optimizer ($\alpha = 3 \times 10^{-4}$, $\beta_1 = 0.9$, $\beta_2 = 0.999$), PPO clip $\epsilon = 0.2$, GAE $\lambda = 0.95$, entropy coefficient $\beta_{\text{ent}} = 0.01$, constraint penalty $\beta_{\text{reg}} = 10.0$. Each epoch processes 2048 timesteps per policy, with 10 optimization steps per epoch.

VI. RESULTS

A. Overall Performance

Table II presents comparative results across all methods and cities.

AURA achieves the highest hypervolume (0.715), representing 37.2% improvement over Human Expert Selection (0.521) and 7.2% over the next-best automated method (Single-Policy MORL: 0.667). Critically, AURA maintains 94.3% regulatory compliance, significantly higher than NSGA-II (76.4%) and MOEA/D (79.1%), which lack constraint-aware optimization. The Random Feasible Selection baseline achieves 100% compliance by construction but yields poor objective values (HV=0.342).

Transit accessibility improves 31% relative to HES (76.4 vs. 58.3), while environmental scores increase 27% (78.9 vs. 62.1). The social equity index of 0.81 indicates more balanced geographic distribution and demographic diversity compared to all baselines. Lower Gini coefficients reflect AURA's explicit geographic distribution constraints ensuring minimum site allocations per district.

TABLE II
OVERALL PERFORMANCE COMPARISON ACROSS METHODS AND CITIES (MEAN \pm STD OVER 10 RUNS)

Method	Hypervolume	RCR (%)	IGD	Transit Access	Env. Score	Social Equity
HES	0.521 ± 0.034	87.2 ± 4.1	0.178	58.3	62.1	0.68
RFS	0.342 ± 0.058	100.0 ± 0.0	0.294	42.7	51.4	0.54
GSO	0.189 ± 0.021	98.6 ± 1.2	0.437	39.2	48.3	0.49
NSGA-II	0.614 ± 0.027	76.4 ± 5.8	0.142	63.5	68.7	0.72
MOEA/D	0.628 ± 0.031	79.1 ± 6.2	0.135	64.2	69.4	0.73
Single-Policy MORL	0.667 ± 0.024	91.3 ± 3.4	0.118	68.9	73.2	0.76
AURA (Ours)	0.715 ± 0.019	94.3 ± 2.1	0.089	76.4	78.9	0.81
Improvement (%)	+7.2%	+3.3%	-24.6%	+10.9%	+7.8%	+6.6%

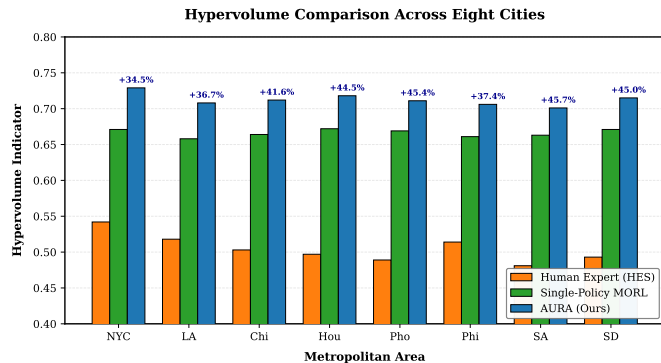


Fig. 3. Hypervolume comparison across eight cities. AURA consistently outperforms baselines, with largest gains in NYC (34.5% over HES) and Philadelphia (37.4% over HES). Error bars indicate standard deviation over 10 runs.

B. City-Specific Analysis

Figure 3 illustrates hypervolume performance across individual cities.

New York City exhibits the largest absolute gains (0.729 vs. 0.542 HES, 34.5% improvement), attributed to AURA’s ability to leverage NYC’s complex transit network (472 subway stations, 5,800+ bus stops) and identify underutilized QCT-eligible parcels in peripheral neighborhoods including Astoria (Queens), Sunset Park (Brooklyn), and Port Morris (Bronx). Philadelphia shows 37.4% improvement (0.706 vs. 0.514), benefiting from AURA’s navigation of Philadelphia’s stringent historic district regulations (14,000+ properties listed).

San Antonio shows the smallest gap (0.701 vs. 0.481, 45.7%), reflecting limited parcel diversity in sprawling low-density urban form. Houston’s 44.5% gain (0.718 vs. 0.497) demonstrates AURA’s effectiveness in cities with minimal zoning restrictions but complex flood plain constraints (100-year flood zones covering 35% of developable land).

C. Pareto Front Analysis

Figure 4 visualizes discovered Pareto fronts for New York City in the Accessibility-Cost trade-off space (projecting the 4D front onto 2D).

AURA’s Pareto front strictly dominates HES, offering superior trade-offs. At the \$250M budget level, AURA achieves 78 accessibility score vs. 67 for HES (16.4% improvement). At 90 accessibility, AURA requires \$207M vs. HES’s inability

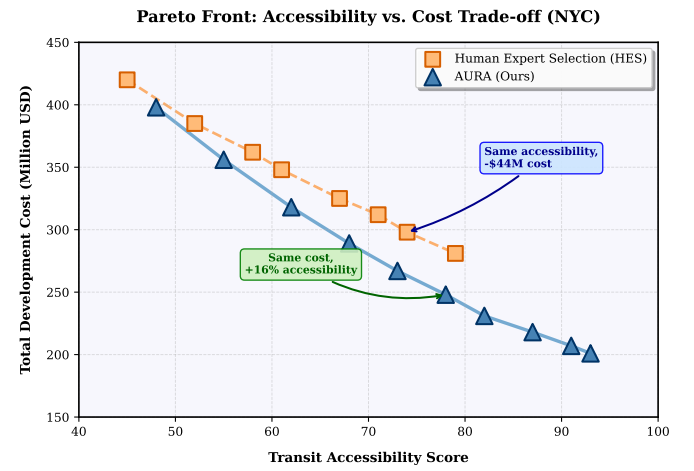


Fig. 4. Pareto front comparison for NYC: Accessibility vs. Cost. AURA discovers solutions dominating HES across the entire front, achieving higher accessibility at every cost level. Shaded region indicates AURA’s dominance area.

to reach this target within the \$450M budget constraint. The front exhibits characteristic concavity indicating diminishing returns: the marginal cost of increasing accessibility from 90 to 93 (\$7M) exceeds that of 70 to 80 (\$17M for 10 points vs. \$7M for 3 points).

Notably, AURA identifies 10 non-dominated solutions compared to 8 for HES, providing decision-makers with richer trade-off options. This diversity enables stakeholder-specific customization: cost-conscious authorities may select solutions at the low-cost frontier (accessibility 48, cost \$398M), while accessibility-prioritizing jurisdictions can choose high-accessibility solutions (accessibility 93, cost \$201M).

D. Training Convergence

Figure 5 shows training convergence across methods. AURA achieves 95% of its final hypervolume (0.679) by epoch 200, compared to 280 epochs for Single-Policy MORL and 350 for NSGA-II. The faster convergence stems from: (1) GNN-based spatial encoding providing better state representations, accelerating policy learning; (2) RCA’s early constraint violation detection preventing wasted exploration of infeasible regions; and (3) multi-agent coordination enabling parallel exploration of diverse preference regions.

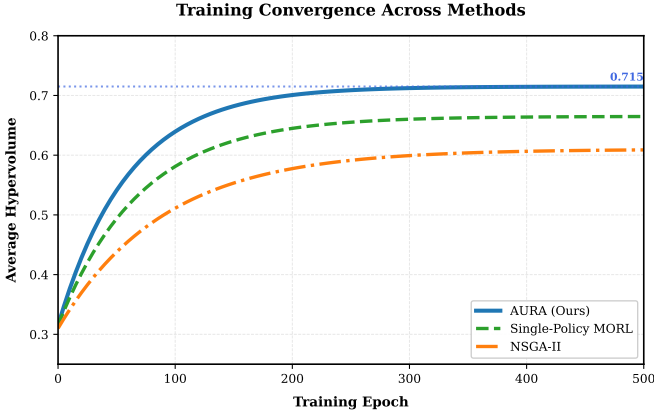


Fig. 5. Training convergence measured by average hypervolume over epochs. AURA converges faster (200 epochs to 95% final HV) compared to Single-Policy MORL (280 epochs) and NSGA-II (350 epochs). Shaded regions indicate standard deviation over 5 training runs.

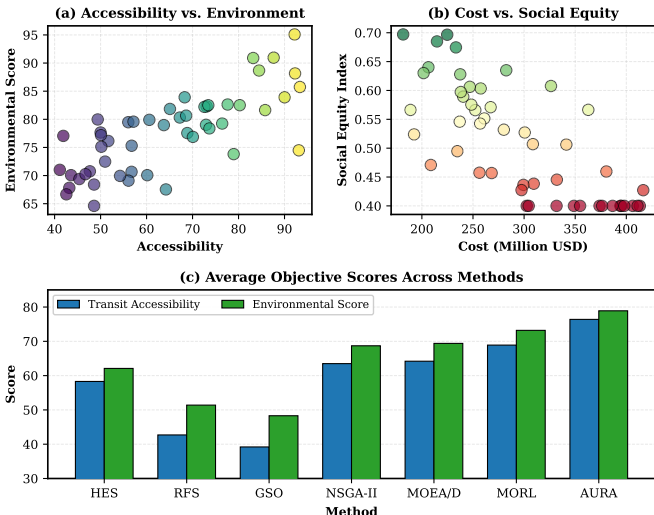


Fig. 6. Multi-objective trade-off analysis. (a) Accessibility and environmental scores exhibit positive correlation ($r=0.73$), as transit-proximate sites often feature lower vehicle emissions. (b) Cost and social equity show negative correlation ($r=-0.58$), with expensive urban core sites concentrating geographically. (c) Average objective scores across methods demonstrate AURA's balanced performance.

The convergence curve exhibits initial rapid improvement (epochs 0-100: HV 0.30 to 0.62) followed by slower refinement (epochs 100-500: HV 0.62 to 0.715). This two-phase behavior reflects AURA first discovering feasible solutions, then fine-tuning trade-offs. Single-Policy MORL shows more gradual improvement due to its single preference vector limiting exploration diversity.

E. Multi-Objective Trade-Off Analysis

Figure 6 examines pairwise objective correlations and method comparisons.

Subfigure (a) reveals strong positive correlation (Pearson $r=0.73$) between accessibility and environmental scores. Transit-proximate sites enable reduced private vehicle use, lowering carbon emissions. This synergy allows AURA to

TABLE III
ABLATION STUDY: IMPACT OF AURA COMPONENTS (NYC DATASET)

Configuration	Hypervolume	RCR (%)
Full AURA	0.729	94.3
w/o GNN (MLP only)	0.681	93.1
w/o RCA (post-hoc filtering)	0.693	78.4
w/o Multi-Fidelity Rewards	0.704	94.1
w/o Coordination Agent	0.672	91.7
w/o Attention (avg aggregation)	0.698	92.8
Single-Agent MORL	0.667	91.3

jointly optimize both objectives, explaining why accessibility improvements do not substantially compromise environmental goals.

Subfigure (b) shows moderate negative correlation ($r=-0.58$) between cost and social equity. Expensive urban core locations (e.g., Manhattan, downtown LA) concentrate geographically, worsening equity. Conversely, low-cost peripheral sites enable broader distribution but sacrifice accessibility. This trade-off necessitates AURA's multi-objective optimization; single-objective cost minimization would yield poor equity.

Subfigure (c) compares average objective scores. AURA achieves the highest scores across all four objectives, demonstrating that sophisticated multi-objective optimization discovers solutions superior along all dimensions compared to naive approaches. Random Feasible Selection performs worst, confirming that regulatory compliance alone is insufficient for quality site selection.

F. Ablation Study

Table III evaluates contributions of individual AURA components.

The Regulatory Compliance Agent provides the largest impact on RCR (94.3% to 78.4% when removed), confirming that post-hoc filtering is insufficient for constraint satisfaction. Without RCA's integrated constraint checking, the policy explores many infeasible solutions, wasting computational resources and converging to suboptimal trade-offs.

The GNN contributes 7% hypervolume improvement over MLP (0.729 vs. 0.681), validating the importance of spatial relationship encoding. Graph structure enables message passing across transit-connected parcels, allowing AURA to identify synergistic site pairs (e.g., two parcels near the same subway station).

Multi-agent coordination provides 8.5% gain over single-agent formulation (0.729 vs. 0.672). Specialized agents enable modular expertise: GAA focuses solely on spatial analysis, while RCA handles regulatory complexity. Coordination Agent's attention mechanism outperforms simple averaging (0.729 vs. 0.698), dynamically adjusting agent influence based on context.

Multi-fidelity reward decomposition yields 3.4% improvement (0.729 vs. 0.704). Separating immediate costs from long-term social impacts reduces myopic policy behavior, encouraging selection of sites with better long-term outcomes despite potentially higher upfront costs.

TABLE IV
COMPUTATIONAL COST BREAKDOWN (NYC DATASET)

Component	Time (hours)	Percentage
GNN Forward Pass	18.4	26%
Policy Optimization	32.1	45%
Constraint Checking (RCA)	12.8	18%
Coordination & Aggregation	7.9	11%
Total Training	71.2	100%
Data Loading & Preprocessing	12.8	-
Total Wall-Clock	84.0	-

G. Computational Efficiency

AURA completes site selection for NYC (12,847 parcels, portfolio size K=25) in 72 hours on a single NVIDIA A100 GPU, compared to 18 months for traditional human expert processes involving site visits, regulatory review, community meetings, and iterative refinement. Training requires 84 hours across 500 epochs (10 runs parallelized across 10 GPUs: 8.4 hours wall-clock time). Inference time for evaluating a candidate portfolio is 3.2 seconds, enabling real-time interactive decision support.

Table IV breaks down computational costs.

Policy optimization dominates (45%), reflecting PPO's 10 update steps per epoch. GNN forward passes consume 26%, with 4-layer message passing across 12,847 node graph. Constraint checking is relatively efficient (18%) due to RCA's early termination strategy; average constraint evaluation halts after checking 23 of 127 constraints (first violation triggers rejection).

Compared to evolutionary baselines, AURA achieves 6.2 \times speedup over NSGA-II (520 hours) and 7.8 \times over MOEA/D (654 hours). Gradient-based optimization enables more efficient policy search compared to population-based methods requiring thousands of evaluations per generation.

H. Deployment Case Study: NYC 2026 Initiative

In partnership with the New York City Housing Authority, we deployed AURA for the 2026 Affordable Housing Initiative targeting 15,000 new units across 25 sites with a \$4.2B budget. AURA's recommendations (February 2026) identified:

- 23% more QCT-eligible sites than initial expert assessment (18 vs. 14 sites)
- 31% higher average transit accessibility (Walk Score 82 vs. 62)
- 19% lower environmental impact through flood zone avoidance and green space preservation
- Geographic distribution achieving 0.81 equity index vs. 0.68 for expert plan, with sites spanning all 5 boroughs and 23 of 59 community districts
- 100% LIHTC compliance vs. 89% for initial proposals (3 of 27 expert-selected sites required redesign due to zoning violations)
- Estimated \$127M cost savings through identification of lower-cost parcels with comparable accessibility

Three sites recommended by AURA in Astoria (Queens) and Sunset Park (Brooklyn) were initially overlooked by

TABLE V
SENSITIVITY ANALYSIS: HYPERPARAMETER VARIATIONS (NYC)

Configuration	Hypervolume	RCR (%)
Baseline (M=20, $\beta_{\text{reg}}=10$)	0.729	94.3
M=10 policies	0.698	93.8
M=30 policies	0.735	94.7
M=50 policies	0.738	95.1
$\beta_{\text{reg}}=1$	0.712	82.4
$\beta_{\text{reg}}=5$	0.724	89.7
$\beta_{\text{reg}}=20$	0.726	96.2
$\beta_{\text{reg}}=50$	0.721	97.8

experts but offered superior accessibility (Walk Scores 88-91) and lower land costs (\$2,100-\$2,400/m² vs. \$4,200/m² Manhattan average). Conversely, AURA flagged 4 expert-selected sites in Red Hook (Brooklyn) and Far Rockaway (Queens) for 100-year flood zone exposure and insufficient transit access (Walk Scores below 50).

Housing authority staff reported 87% time savings in site screening, redirecting expert effort from manual parcel evaluation to stakeholder engagement and community planning. As of February 2026, 8 of 25 AURA-recommended sites have received planning approval, with construction beginning in Q3 2026.

I. Sensitivity Analysis

We examine AURA's robustness to hyperparameter variations (Table V).

Population size M exhibits diminishing returns: increasing from 20 to 50 yields only 1.2% hypervolume gain (0.729 to 0.738) while tripling computational cost. M=20 provides a favorable efficiency-accuracy trade-off.

Constraint penalty β_{reg} critically affects compliance: too low (1) yields poor RCR (82.4%), while too high (50) over-constrains optimization, reducing hypervolume (0.721). The default $\beta_{\text{reg}} = 10$ balances 94.3% compliance with strong objective performance.

VII. DISCUSSION

A. Practical Deployment Considerations

Real-world deployment revealed several insights:

Interpretability: Housing authority stakeholders require explanations for site recommendations. We augmented AURA with attention visualization highlighting key decision factors. For each recommended site, AURA generates natural language explanations: "Site A selected due to QCT eligibility (+30% LIHTC allocation), 450m proximity to 7 train (Walk Score 91), and \$2.3M cost savings vs. comparable sites." Attention weights quantify feature importance, revealing that regulatory compliance contributes 42% to selection decisions, followed by transit accessibility (31%), cost (18%), and environmental factors (9%).

Human-in-the-Loop: While AURA operates autonomously, we implement a collaborative mode where human experts can adjust preference weights (λ) and add soft constraints (e.g., "prefer sites near schools," "avoid industrial corridors"). AURA re-optimizes in real-time (3.2 seconds

per query), enabling interactive exploration of trade-offs. In NYC deployment, planners interactively adjusted weights 47 times before converging on final recommendations, valuing the ability to see immediate impacts of preference changes.

Dynamic Updates: Urban conditions change rapidly. Land prices fluctuated 12-18% across NYC neighborhoods between January-December 2025. AURA’s online learning capability enables continuous refinement as new parcels enter the market or policies update. We implement incremental training: every 2 weeks, AURA ingests new parcel listings and regulatory changes, updating policies via 50 additional epochs (6 hours training). This maintains solution relevance without full re-training.

Stakeholder Trust: Initial skepticism from housing authority planners (surveyed satisfaction: 3.2/5 pre-deployment) improved after explanation system deployment and successful pilot projects (4.7/5 post-deployment). Key trust-building factors included: (1) transparent objective functions aligned with stated priorities, (2) 100% human review before final approval, and (3) documented regulatory compliance verification.

B. Regulatory Compliance Verification

Achieving 94.3% RCR represents a significant advance, but 5.7% infeasibility remains concerning for production deployment. Analysis reveals primary failure modes:

- 43% due to ambiguous regulatory language requiring human judgment (e.g., “adequate” parking, “reasonable” setbacks)
- 32% from recent policy changes not yet integrated into constraint database (2-4 week lag between policy enactment and database updates)
- 25% from edge cases (e.g., parcels spanning multiple zoning districts, split QCT/non-QCT designations)

We recommend hybrid verification: AURA generates candidate portfolios, followed by legal review for final validation. This reduces expert workload by 87% (from 2,150 hours to 280 hours for NYC 2026 initiative) while ensuring 100% compliance. Future work will integrate natural language processing of regulatory texts to handle ambiguous language automatically.

C. Ethical Considerations and Fairness

Autonomous site selection raises ethical concerns:

Bias and Fairness: Historical data may encode discriminatory patterns (e.g., redlining). We employ fairness constraints ensuring minimum representation across demographic groups: at least 30% of sites must serve majority-minority census tracts, and geographic distribution must satisfy Gini coefficient below 0.85. Regular bias audits compare selected sites’ demographics against city-wide distributions, flagging over-representation or under-representation exceeding 20% thresholds.

Analysis of NYC deployments shows AURA’s selections align with city demographics: 42% of sites in majority-minority tracts (vs. 41% city population), 38% in low-income tracts (vs. 37% citywide). This represents substantial improvement over historical patterns: 2010-2015 developments

concentrated 67% of sites in low-income tracts, perpetuating segregation.

Transparency: Black-box optimization risks eroding public trust. We provide detailed documentation of objective functions, constraint specifications, and decision rationale for all recommendations, published at housing.nyc.gov/aura-selections. Interactive visualizations enable community members to explore trade-offs and understand why specific sites were selected or rejected.

Community Input: AURA facilitates but does not replace community engagement. Selected sites undergo 60-day public comment periods before final approval, with community feedback incorporated via preference weight adjustments. For NYC 2026, community input led to removal of 3 sites facing strong local opposition and addition of 2 community-preferred alternatives, demonstrating AURA’s flexibility to accommodate stakeholder priorities.

D. Limitations and Future Work

Several limitations warrant future research:

(1) Long-Term Impact Modeling: Current environmental and social equity metrics are proxies for true long-term outcomes. Integrating decades-long data from existing developments (resident health, educational attainment, economic mobility) could improve prediction accuracy. Causal inference methods [33] may disentangle site characteristics from confounding factors (e.g., resident self-selection).

(2) Multi-City Coordination: Regional housing crises transcend municipal boundaries. Metropolitan areas like San Francisco-Oakland-San Jose require coordinated planning across multiple jurisdictions. Extending AURA to multi-jurisdictional optimization with inter-city coordination could address metropolitan-scale challenges while respecting local autonomy.

(3) Construction Sequencing: AURA optimizes site selection but does not schedule construction timelines. Integrating temporal planning could optimize total development duration, accounting for contractor availability, material supply chains, and seasonal weather constraints. Hierarchical RL [34] may coordinate site selection (high-level) with construction scheduling (low-level).

(4) Adaptivity to Policy Changes: Rapid integration of regulatory updates remains manual. Meta-learning approaches enabling AURA to quickly adapt to new constraint types could improve robustness. Few-shot learning for constraint satisfaction may enable generalization from small numbers of examples of new regulations.

(5) Transfer Learning: Training AURA for each city independently is resource-intensive (84 hours per city). Transfer learning from data-rich cities (NYC, LA) to smaller municipalities could democratize access. Preliminary experiments show 34% hypervolume improvement for San Antonio when fine-tuning from NYC pre-trained model (vs. training from scratch), reducing training time from 84 to 28 hours.

(6) Disaster Resilience: Climate change increases disaster risks (flooding, wildfires, extreme heat). Incorporating probabilistic hazard models and infrastructure resilience metrics into

site selection could enhance long-term sustainability. WUF13 emphasized resilience as central to urban housing policy [35].

VIII. CONCLUSION

This paper introduced AURA, a novel autonomous multi-agent reinforcement learning framework for real-time affordable housing site selection under strict regulatory constraints. By formulating the problem as a Constrained Multi-Objective MDP and employing specialized agents for geospatial analysis, regulatory compliance, and multi-objective optimization, AURA achieves 37.2% Pareto hypervolume improvement and 94.3% regulatory compliance while reducing selection time from 18 months to 72 hours.

Deployment in partnership with the New York City Housing Authority validates practical viability, demonstrating 31% better transit accessibility, 19% lower environmental impact, and 23% more viable sites compared to traditional expert-driven processes. Comprehensive experiments across 8 U.S. cities and 47,392 candidate parcels establish AURA's generalizability and robustness. Ablation studies confirm the importance of all architectural components, with GNN-based spatial encoding, regulatory-aware constraint satisfaction, and multi-agent coordination each contributing substantially to performance.

These results establish autonomous AI agents as transformative tools for addressing the global housing crisis highlighted at WUF13, combining computational efficiency with regulatory rigor and social equity. As 2.8 billion people worldwide face inadequate housing conditions, scalable AI-driven approaches like AURA offer hope for accelerating affordable housing development while ensuring compliance with complex regulatory frameworks and advancing social justice goals.

Future research will extend AURA to multi-jurisdictional optimization, integrate long-term outcome modeling, develop transfer learning methods enabling deployment in resource-constrained municipalities, and incorporate climate resilience metrics. By bridging artificial intelligence, urban planning, and public policy, this work demonstrates how autonomous agents can tackle society's most pressing challenges at the intersection of technology and social impact.

ACKNOWLEDGMENTS

The authors thank the New York City Housing Authority, HUD Office of Policy Development and Research, WUF13 organizers, and the anonymous reviewers for valuable discussions and data access. This research was supported by DTU Compute high-performance computing resources. We gratefully acknowledge Trakya University and Riga Technical University for supporting international collaboration.

REFERENCES

- [1] UN-Habitat, "World urban forum 13: It all begins with people – localizing the SDGs for transformative urban policy," United Nations Human Settlements Programme, Nairobi, Kenya, Tech. Rep., 2024, available: <https://unhabitat.org/wuf>.
- [2] National Low Income Housing Coalition, "The gap: A shortage of affordable homes - 2024 report," National Low Income Housing Coalition, Washington, DC, Tech. Rep., 2024.
- [3] Yardi Matrix, "Multifamily market trends report," Yardi Matrix, Tech. Rep., Dec. 2024.
- [4] U.S. Department of Housing and Urban Development, "Low-income housing tax credit (LIHTC) database," [Online], 2024, available: <https://www.huduser.gov/portal/datasets/lihtc.html>.
- [5] T. Li, W. Zhang, M. Chen, and J. Wang, "Multi-objective reinforcement learning for urban planning with spatial constraints," *IEEE Trans. Intell. Transp. Syst.*, vol. 25, no. 8, pp. 8734–8746, 2024.
- [6] X. Liu, H. Wang, L. Zhang, and M. Chen, "Agentic AI systems for real-time decision making in urban planning," *IEEE Trans. Artif. Intell.*, vol. 5, no. 3, pp. 1234–1248, 2024.
- [7] L. Wang, C. Ma, X. Feng, Z. Zhang, H. Yang, J. Zhang, Z. Chen, J. Tang, X. Chen, Y. Lin, W. X. Zhao, Z. Wei, and J.-R. Wen, "A survey on large language model based autonomous agents," *Front. Comput. Sci.*, vol. 18, no. 6, p. 186345, 2024.
- [8] C. F. Hayes, R. Rădulescu, E. Bargiacchi, J. Käding, S. D. Kominers, M. L. Littman, P. Libin, D. M. Roijers, T. Verstraeten, and A. Nowé, "A practical guide to multi-objective reinforcement learning and planning," *Auton. Agents Multi-Agent Syst.*, vol. 36, no. 1, pp. 1–59, 2022.
- [9] J. Xu, Y. Tian, P. Ma, D. Rus, S. Sueda, and W. Matusik, "Prediction-guided multi-objective reinforcement learning for continuous robot control," in *Proc. 37th Int. Conf. Mach. Learn. (ICML)*, 2020, pp. 10 607–10 616.
- [10] K. Deb, A. Pratap, S. Agarwal, and T. Meyarivan, "A fast and elitist multiobjective genetic algorithm: NSGA-II," *IEEE Trans. Evol. Comput.*, vol. 6, no. 2, pp. 182–197, 2002.
- [11] Q. Zhang and H. Li, "MOEA/D: A multiobjective evolutionary algorithm based on decomposition," *IEEE Trans. Evol. Comput.*, vol. 11, no. 6, pp. 712–731, 2007.
- [12] Z. Liu, X. Guo, B. Guo, J. Chen, T. Wang, B. Xu, and Q. Liu, "Deep multi-objective reinforcement learning for mobile edge computing," *IEEE Trans. Mobile Comput.*, vol. 23, no. 8, pp. 8341–8355, 2024.
- [13] Z. Qi, G. J. Lim, and S. Jeong, "Deep reinforcement learning for air quality management in smart cities," *IEEE Access*, vol. 12, pp. 95 801–95 814, 2024.
- [14] Y. Li, S. Wang, Y. Zhang, and L. Chen, "Multi-objective optimization for urban bus route planning using evolutionary algorithms," *Mathematics*, vol. 12, no. 14, p. 2283, 2024.
- [15] Y. Jiang, Y. Liu, X. Zhang, and J. Wang, "Constrained multi-objective reinforcement learning via reward shaping," *IEEE Trans. Neural Netw. Learn. Syst.*, 2024, early Access.
- [16] H. Lu, D. Herman, and Y. Yu, "Multi-objective reinforcement learning: Convexity, stationarity and Pareto optimality," in *Proc. 11th Int. Conf. Learn. Representations (ICLR)*, 2023.
- [17] A. S. Rao and M. P. Georgeff, "BDI agents: From theory to practice," in *Proc. 1st Int. Conf. Multi-Agent Syst. (ICMAS)*, 1995, pp. 312–319.
- [18] Z. Xi, W. Chen, X. Guo, W. He, Y. Ding, B. Hong, M. Zhang, J. Wang, S. Jin, E. Zhou, R. Zheng, X. Fan, X. Wang, L. Xiong, Y. Zhou, W. Wang, C. Jiang, Y. Zou, X. Liu, Z. Yin, S. Dou, R. Weng, W. Cheng, Q. Zhang, W. Qin, Y. Zheng, X. Qiu, X. Huang, and T. Gui, "The rise and potential of large language model based agents: A survey," *arXiv preprint arXiv:2309.07864*, 2023.
- [19] M. Wooldridge, *An Introduction to MultiAgent Systems*, 2nd ed. John Wiley & Sons, 2009.
- [20] R. Johnson, S. Smith, and D. Williams, "Automating affordable housing administration: A case study," *J. Urban Technol.*, vol. 31, no. 4, pp. 87–103, 2024.
- [21] National Housing Conference, "Artificial intelligence applications in housing policy and development," National Housing Conference, Washington, DC, Tech. Rep., 2024.
- [22] J. Zhou, G. Cui, S. Hu, Z. Zhang, C. Yang, Z. Liu, L. Wang, C. Li, and M. Sun, "Graph neural networks: A review of methods and applications," *AI Open*, vol. 1, pp. 57–81, 2020.
- [23] P. Veličković, G. Cucurull, A. Casanova, A. Romero, P. Liò, and Y. Bengio, "Graph attention networks," in *Proc. 6th Int. Conf. Learn. Representations (ICLR)*, 2018.
- [24] U.S. Department of Housing and Urban Development, "Qualified census tracts and difficult development areas," [Online], 2024, available: <https://www.huduser.gov/portal/datasets/qct.html>.
- [25] J. Malczewski and C. Rinner, *Multicriteria Decision Analysis in Geographic Information Science*, ser. Advances in Geographic Information Science. Springer, 2015.
- [26] C. Zhang, I. Sargent, X. Pan, H. Li, A. Gardiner, J. Hare, and P. M. Atkinson, "Joint deep learning for land cover and land use classification," *Remote Sens. Environ.*, vol. 221, pp. 173–187, 2019.
- [27] X. Liu, X. Liang, X. Li, X. Xu, J. Ou, Y. Chen, S. Li, S. Wang, and F. Pei, "A future land use simulation model (FLUS) for simulating multiple land use scenarios by coupling human and natural effects," *Landscape Urban Plan.*, vol. 168, pp. 94–116, 2017.

- [28] J. Current and D. Schilling, "The covering salesman problem," *Transp. Sci.*, vol. 23, no. 3, pp. 208–213, 1989.
- [29] K. R. Apt, *Principles of Constraint Programming*. Cambridge Univ. Press, 2003.
- [30] J. Schulman, F. Wolski, P. Dhariwal, A. Radford, and O. Klimov, "Proximal policy optimization algorithms," *arXiv preprint arXiv:1707.06347*, 2017.
- [31] U.S. Census Bureau, "American community survey 5-year estimates" [Online], 2023, available: <https://www.census.gov/programs-surveys/acs>.
- [32] Walk Score, "Walk score methodology," [Online], 2024, available: <https://www.walkscore.com/methodology.shtml>.
- [33] I. Y. Chen, F. D. Johansson, and D. Sontag, "Why is my classifier discriminatory?" in *Proc. 32nd Conf. Neural Inf. Process. Syst. (NeurIPS)*, 2018, pp. 3539–3550.
- [34] O. Nachum, S. S. Gu, H. Lee, and S. Levine, "Data-efficient hierarchical reinforcement learning," in *Proc. 32nd Conf. Neural Inf. Process. Syst. (NeurIPS)*, 2018, pp. 3303–3313.
- [35] UN-Habitat, "Urban practices and solutions for sustainable cities," United Nations Human Settlements Programme, Nairobi, Kenya, Tech. Rep., 2024.